EPJ Web of Conferences **356**, 01004 (2026) https://doi.org/10.1051/epjconf/202635601004
ICC 2025

Formation of Nanocrystalline ferrite: Effect of Citric Acid on Structural and Spectroscopic Properties

Yashpal Choudhary[1], *Shobha Ram Choudhary*[1], *P.M. Saini*[1], *Ritu*[1] *P. A. Alvi*[1], *B. L. Choudhary*[1*]
[1]*Department of Physics, Banasthali Vidyapith, Banasthali-304022, Rajasthan, India*

Abstract. Nanocrystalline $Co_{0.1}Ni_{0.7}Zn_{0.2}Fe_2O_4$ ferrite nanoparticles were synthesized via the sol–gel method to investigate the influence of citric acid concentration on their structural and spectroscopic properties. X-ray diffraction confirmed the formation of a single-phase cubic spinel structure with well-defined reflections corresponding to the (220), (311), (400), (422), (511), and (440) planes. The crystallite size, estimated using Scherrer's equation, was found to increase from ~7.5 nm to ~21 nm with increasing citric acid content, indicating a strong correlation between chelating agent concentration and particle growth. Lattice parameters, dislocation density, unit cell volume, hopping lengths, and bond lengths were systematically evaluated, revealing modifications in lattice strain and structural ordering. Williamson–Hall analysis further demonstrated the presence of microstrain induced by size effects and lattice imperfections, with strain values varying as a function of citric acid concentration. FTIR spectroscopy exhibited characteristic metal–oxygen stretching vibrations associated with tetrahedral and octahedral sites, validating the formation of the spinel ferrite lattice, along with minor organic residue-related bands originating from the sol–gel process. The combined structural and spectroscopic analyses confirm that citric acid plays a crucial role in controlling crystallite size, lattice strain, cation distribution, and bonding characteristics in the synthesized ferrite system. These findings highlight the importance of chelating agent concentration in tailoring the structural integrity and physicochemical behavior of Co–Ni–Zn ferrite nanoparticles for potential technological and functional applications.

1 Introduction

Magnetic nanoparticles are now considered as a very important area of research that is mainly due to their size-dependent physical and magnetic properties. When the particles are of very small sizes, less than what is called a critical limit, then the first behavior which is multi-domain gets changed to a single domain and this leads to a more considerable reduction of saturation magnetization, increasing coercivity, and lowering magnetic anisotropy [1–4]]. The external factors at such a small scale would be the surface area and the finite size, which

* Corresponding author: blcphysics@gmail.com

would have a strong influence on the magnetic response. There is a given relationship between particle size and magnetic properties. Besides, the smaller the particle the larger the surface-to-volume ratio gets, which consequently leads to more surface disorder and altered spin interactions, besides the fact that the optical, structural and vibrational properties of the material would be affected as well. That is why the control of the size of the particles is vital for the nanoparticles' performance to be optimized. Magnetic nanomaterials, spinel ferrites have drawn the most awareness due to their chemical stability and tunable properties. These kinds of materials are characterized by the general formula AFe_2O_4 ($A = Co^{2+}, Ni^{2+}, Zn^{2+}$) and their cubic spinel structure ($Fd\bar{3}m$) where both tetrahedral and octahedral sites are filled with the metal cations [5–8]. The redistribution of cations among the different sites will have a great impact on the superexchange interactions and thus affect the optical and magnetic properties of our material. The charge neutrality in the substituted ferrites is upheld through Fe^{3+}/Fe^{2+} conversion and the creation of oxygen-related defects among others. The defects create localized states which influence the material's electrical conductivity, optical band gap, lattice strain, and vibrational characteristics, this could be done through analyzing with XRD and FTIR techniques. The spinel ferrite nanoparticles are extensively used in the areas mentioned above because of their customizable properties, data storage, and permanent magnets, sensors, microwave, and medical applications.

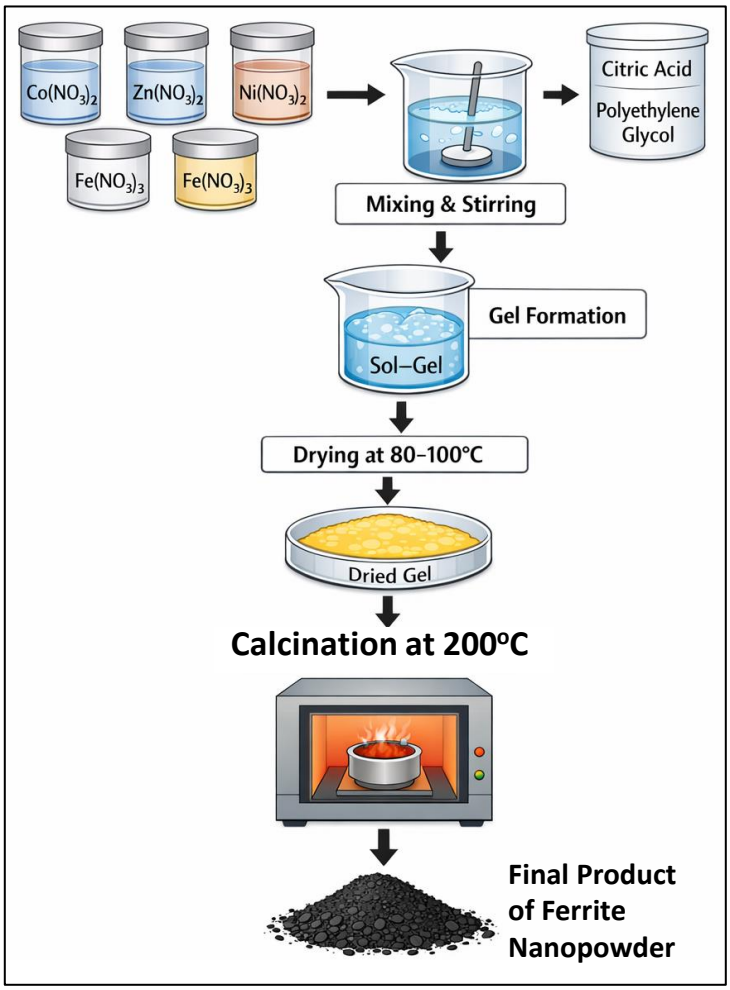

Fig. 1. Synthesis process of $Co_{0.1}Zn_{0.7}Ni_{0.2}Fe_2O_4$ for different citric acid concentrations.

In the present work, $Co_{0.1}Ni_{0.7}Zn_{0.2}Fe_2O_4$ ferrite nanoparticles were composed using the sol–gel auto combustion method, which is known for its excellent compositional homogeneity, low processing temperature, and precise control over particle size. The impact of citric acid on the structural and optical properties of the synthesized samples has been systematically examined. The composed samples were characterized by XRD to confirm phase formation, crystallinity, and structural parameters. Additionally, FTIR spectra was employed showed characteristic metal–oxygen vibrations [9–15].

2 Sample preparation

The sol-gel technique was employed to produce the ferrites $Co_{0.1}Ni_{0.7}Zn_{0.2}Fe_2O_4$. Initially, a completely transparent solution was made by dissolving all the metal nitrates in DI water [8-9]. The liquid was continuously agitated with a magnetic stirrer after the addition of citric acid as a chelating agent. Dropwise addition of ammonia (NH_3) solution was done to bring the pH up to a value in the range of 8 to 10. The gel formation took place gradually with constant stirring as the temperature was raised[16] . A gel would look like burnt ashes. The black ash-like material was ground finely with a mortar and pestle after drying [16,17].

3 Results and discussion

3.1 XRD

X-ray diffraction is certainly a powerful techniques to determine, among others, the material's phase purity and structure. The present work involved the X-ray diffraction of ferrite nanoparticles carried out at room temperature with the overall angle of 2θ ranging from 20º to 70º. The X-ray diffraction pattern of ferrite nanoparticles exhibited very well the reflections (220), (311), (222), (400), (422), (511), and (440) that belong to the spinel cubic structure of the strong type[9,12,18,19]. From the height of the prominent (311) peak, different parameters related to XRD were extracted. The analysis of the XRD pattern reveal that the synthesized nano ferrite had a spinel cubic single-phase structure. The structural parameters were obtained from the XRD data collected. The crystallite size (D) was estimated using the Scherrer's formula which is calculated by :

$$D = 0.89\lambda/\beta\cos\theta \quad (1)$$

D represents crystallite size, β is FWHM, and λ is wavelength ,while θ corresponds to the Bragg angle in XRD. The second equation was used to estimate the lattice constant for the ferrite nanoparticles .

$$a = d_{hkl}(h^2 + k^2 + l^2)^{1/2} \quad (2)$$

Here a is the lattice parameter and dhkl is used to indicate the distance between the nearest planes. Additionally, standard relations were applied to calculate dislocation density and unit cell volume (V) as other structural parameters[7,20–22]. The structural parameter values are compiled in table 1.

Table 1 comprises the calculated following values extracted from the XRD pattern.

Citric Acid(gm)	Peak Position (degree)	Crystallite Size(nm)	Lattice Parameter [Å]	Volume $[Å]^3$	Dislocation density
0.5	35.36	7.5	8.41	594.8	1.78×10^{16}
1	35.50	11.1	8.40	592.7	8.11×10^{15}
1.5	35.61	11.8	8.35	582.0	7.18×10^{15}
2	35.33	21.3	8.42	596.7	2.20×10^{15}

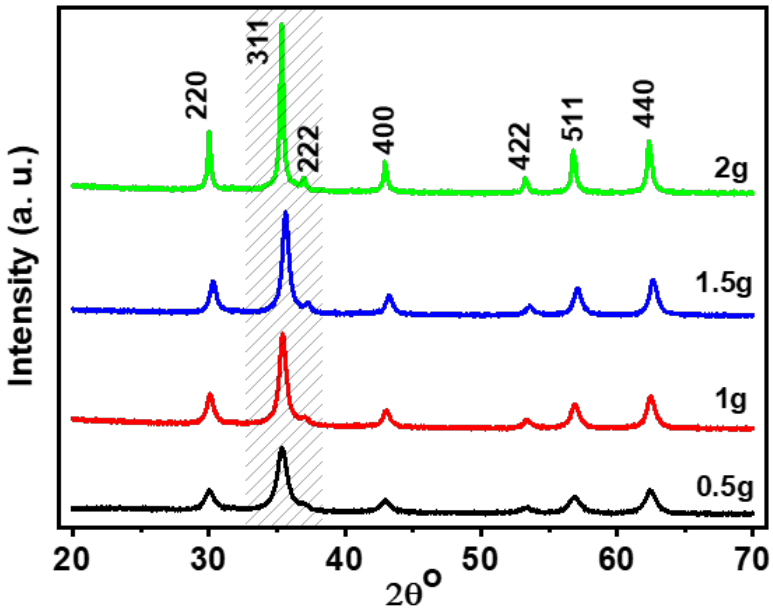

Fig. 2. XRD spectra of $Co_{0.1}Zn_{0.7}Ni_{0.2}Fe_2O_4$ for different citric acid concentrations.

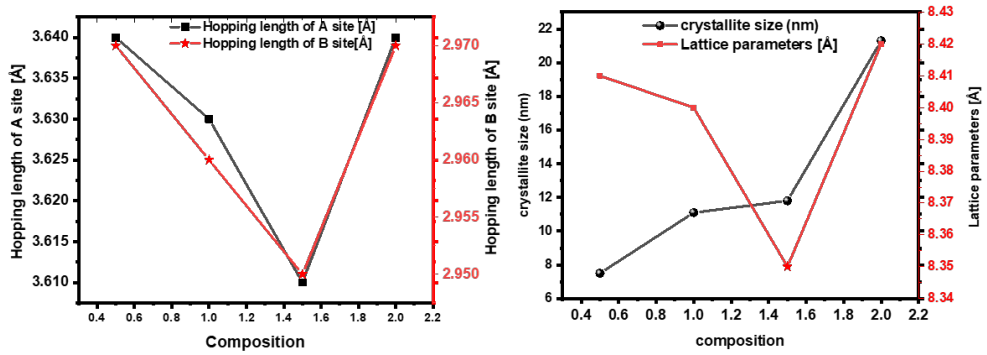

Fig.3. Demonstrated the variation in hopping length of side A and B with the citric acid composition and the changes observed in crystallite size and lattice parameters.

3.2 W-H Plot

The micro strain (ε) was estimated by applying the Williamson–Hall (W–H) method, which establishes a connection between the size of crystallites (D) and peak broadening caused by lattice distortion.

$$\alpha\ \beta cos\theta = 0.9\lambda/D + 4\varepsilon sin\theta \quad (3)$$

In this technique, λ represents X-ray wavelength, β is FWHM measured in radians, 0.9 is chosen as the shape factor, and ε stands for the strain in the produced material. The lattice strain was calculated from the W–H plot by placing 4sinθ on x-axis and βcosθ on y-axis Figure4[17,20,23]. The micro strain values for all samples were obtained from these plots and are recorded in Table 2.

Table 2: summarizes the evaluated values extracted from the XRD patterns.

Citric Acid(gm)	L_A [Å]	L_B [Å]	Micro strain	d_{AX} [Å]	d_{BX} [Å]
0.5	3.64	2.97	0.00273	1.82	3.41
1	3.63	2.96	0.00447	1.81	3.40
1.5	3.61	2.95	0.00339	1.80	3.38
2	3.64	2.97	0.00766	1.82	3.41

L_A and L_B are determined from the following relations :

$$L_A = 0.25\, a \sqrt{3} \qquad L_B = 0.25\, a \sqrt{2} \tag{4}$$

Where, L_A and L_B denoted to the hopping length for A and B sites, respectively. Given that the have various ionic radii, such as octahedral and tetrahedral bond length d_{AX}(Å) and d_{BX}(Å) are explained as :

$$d_{AX}(Å) = \sqrt[a]{3}\,(u - \tfrac{1}{4}) \tag{5}$$

$$d_{BX}(Å) = \sqrt[a]{3}\,u^2 - 2u + 0.375 \tag{6}$$

According to review of literature, the oxygen positional parameter (u) is found to be 0.375.

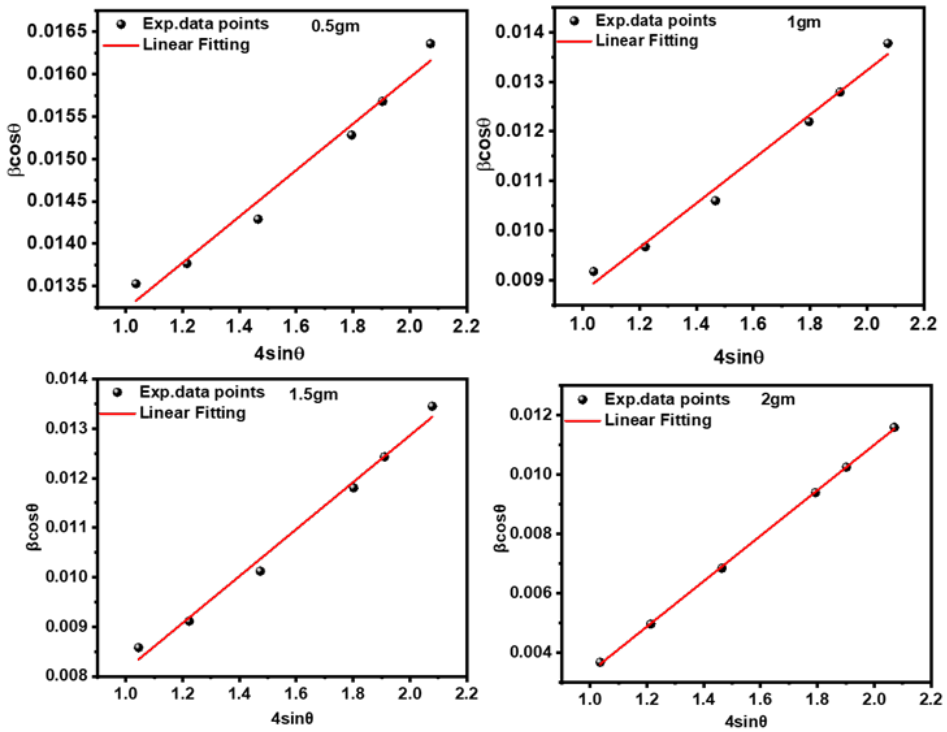

Fig.4. W-H Polt of $Co_{0.1}Zn_{0.7}Ni_{0.2}Fe_2O_4$ for different citric acid concentrations.

3.3 FTIR:

The FTIR spectroscopy has been a tool through which molecular dynamics have been studied. In the case of $Co_{0.1}Zn_{0.7}Ni_{0.2}Fe_2O_4$ with varying in citric acid, this approach is applied not only to the material's structure but also to the functional groups and modes of bonding

present. The functional groups and their characteristic peaks are identified by analyzing the infrared transmittance spectra of the sample powders. The FTIR spectrum of the synthesized samples is within the range of 4000-400cm^{-1}. The spectra exhibit characteristic absorption bands which shows the formation of a cubic spinel ferrite structure[15,24]. The crucial absorption band seen at around 634 cm^{-1} is regarded as the fundamental stretching vibration of the metal-oxygen bonds at the tetrahedral (A) sites of the spinel structure. The other band seeming close to 690 cm^{-1} could be interpreted as the shifted tetrahedral M-O vibrations, resultant from the simultaneous presence of Co^{2+}, Ni^{2+}, and Zn^{2+} ions. The new distribution of cations and the resulting lattice distortion are the reasons for the upward trend in the absorption. These vibrations, along with the band at 690 cm^{-1}, verify that the spinel ferrite phase has been made successfully. The bands at ~1440 cm^{-1} and ~1522 cm^{-1} are, respectively, corresponding to the C–O and C=C/NO_3^- bond stretching. Such a relation is due to organic compounds that were left behind or nitrate preceding during the sol-gel method[6,7,9,25]. The band at ~1579 cm^{-1} is due to the asymmetrical stretching of carboxylate (COO^-) indicating that the chelating agent used was not completely oxidized during calcination. A faint band at ~2329 cm^{-1} was interpreted as the stretching of O=C=O (carbon dioxide), which comes from either enslaved atmospheric CO_2 or gases that are locked in the nanoparticle's porous structure. In general, the FTIR spectrum has revealed the presence of a spinel ferrite structure while indicating the existence of organic residues by the minor peaks. The lack of other impurity peaks points to the very high purity of the cobalt-nickel-zinc ferrite nanoparticles produced[15–17,22,23,26].

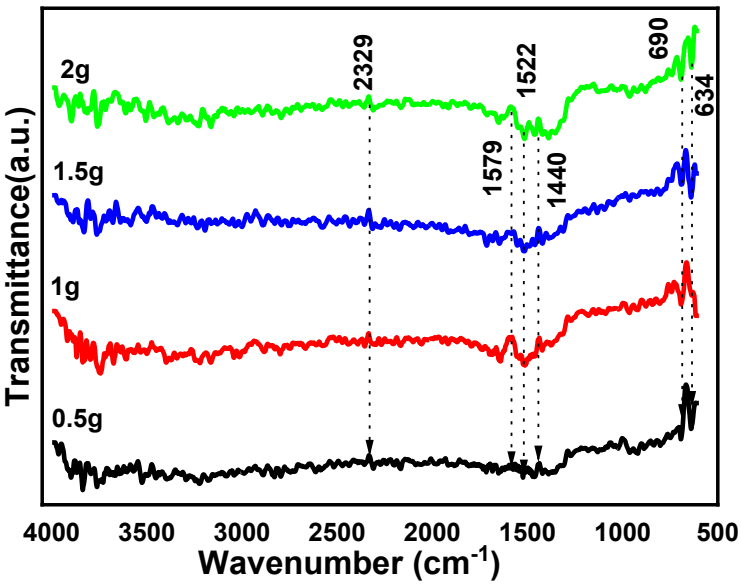

Fig.5. FTIR spectra of $Co_{0.1}Zn_{0.7}Ni_{0.2}Fe_2O_4$ for different citric acid concentrations.

Conclusions

The study successfully produced the nanoferrites of the composition $Co_{0.1}Ni_{0.7}Zn_{0.2}Fe_2O_4$ for for different citric acid concentrations by the sol-gel technique. The XRD analysis revealed the structural properties of obtained samples. The FWHM method was applied to study the peak widening of the nanoparticles leading to lattice strain. The crystallite size was noted to

increased with the citric acid concentratation increases from about 7.5 to 21 nm. The Williamson–Hall plot further enabled the evaluation of lattice microstrain, revealing the presence of residual strain within the crystal lattice arising from size effects and lattice imperfections. FTIR spectra showed characteristic metal–oxygen stretching vibrations equivalent to tetrahedral and octahedral sites, confirming the formation of the ferrite lattice. These results demonstrate that citric acid concentration represents a significant role in controlling crystallite size, microstrain, and bonding characteristics of prepared ferrite nanoparticles.

References

1. S.R. Choudhary, Anchal, K. Choudhary, N. Jakhar, Y. Choudhary, P.A. Alvi, B.L. Choudhary, Tailoring antimicrobial activity through Ni2+ substitution in Cu–Zn ferrite nanoparticles, Mater Chem Phys 349 (2026) 131727. https://doi.org/https://doi.org/10.1016/j.matchemphys.2025.131727.
2. J. Feng, R. Xiong, L. Cheng, Y. Liu, Effect of Chromium Substitution on Structural and Magnetic Properties of Nickel-Cobalt Ferrite Nanoparticles Synthesized by Co-precipitation Method, J Supercond Nov Magn 30 (2017) 3513–3521. https://doi.org/10.1007/s10948-017-4160-z.
3. S. Chakrabarty, S. Bandyopadhyay, M. Pal, A. Dutta, Sol-gel derived cobalt containing Ni–Zn ferrite nanoparticles: Dielectric relaxation and enhanced magnetic property study, Mater Chem Phys 259 (2021) 124193. https://doi.org/https://doi.org/10.1016/j.matchemphys.2020.124193.
4. Sarita, Anchal, S.R. Choudhary, Y. Choudhary, P.K. Bhamu, J. Pandey, M.S.L. Hudson, S.N. Dolia, P.A. Alvi, B.L. Choudhary, Multifaceted characterization of Mn-Doped nanocrystalline NiFe2O4 ferrites, Journal of the Korean Physical Society (2025). https://doi.org/10.1007/s40042-025-01514-3.
5. K.K. Palsaniya, S.R. Choudhary, P.M. Saini, Anchal, S.N. Dolia, P.A. Alvi, B.L. Choudhary, Synthesis and Characterization of Nanocrystalline MgFe2O4 for Multifaceted Applications, Journal of Condensed Matter 2 (2025) 78–80. https://doi.org/10.61343/jcm.v2i02.67.
6. K.K. Palsaniya, Anchal, Sarita, M.S. Rulaniya, P. Yadav, R.K. Beniwal, N. Kumari, P.A. Alvi, B.L. Choudhary, Cobalt Concentration-Dependent Structural and Magnetic Transitions in Nanocrystalline Ni0.9−xZn0.1CoxFe2O4 Ferrites, J Low Temp Phys (2025). https://doi.org/10.1007/s10909-025-03299-y.
7. R. Beniwal, Anchal, P. Yadav, Y. Choudhary, A. Rundla, K. Singh, P.A. Alvi, B.L. Choudhary, Tunable magnetic and structural properties of CrxCo1-xFe2O4 nanoferrites, J Magn Magn Mater 628 (2025) 173186. https://doi.org/https://doi.org/10.1016/j.jmmm.2025.173186.
8. H. Cheema, S. Kumar, P.A. Alvi, B.L. Choudhary, U. Kumar, Synthesis and physical properties of nanopowder and electrical properties of bulk samples of ZnFe2-xNixO4 (x: 0, 0.05, 0.10), Advanced Powder Technology 31 (2020) 4241–4252. https://doi.org/10.1016/j.apt.2020.09.001.
9. S.K. Jain, S.N. Dolia, B.L. Choudhary, B.L. Prashant, Structural and morphological study of Zn0.9Mn0.05Fe0.05O synthesized by sol-gel wet chemical precipitation route, in: IOP Conf Ser Mater Sci Eng, 2018. https://doi.org/10.1088/1757-899X/348/1/012004.
10. B.L. Choudhary, S. Kumar, A. Krishnamurthy, B.K. Srivastava, Preparation and magnetic studies of Mn substituted analogues of BiFeO3, in: AIP Conf Proc, 2011: pp. 83–86. https://doi.org/10.1063/1.3644422.

11. B.L. Choudhary, N. Kumari, J. Kumari, A. Kumar, S.N. Dolia, Relaxation mechanism in Ni0.5Zn0.5Fe2O4 nanocrystalline ferrite at a lower temperature, Mater Lett 304 (2021). https://doi.org/10.1016/j.matlet.2021.130731.
12. B.L. Choudhary, U. Kumar, S. Kumar, S. Chander, S. Kumar, S. Dalela, S.N. Dolia, P.A. Alvi, Irreversible magnetic behavior with temperature variation of Ni0.5Co0.5Fe2O4 nanoparticles, J Magn Magn Mater 507 (2020). https://doi.org/10.1016/j.jmmm.2020.166861.
13. G. Lal, K. Punia, H. Bhoi, S.N. Dolia, B.L. Choudhary, P.A. Alvi, S. Dalela, S.K. Barbar, S. Kumar, Exploring the structural, elastic, optical, dielectric and magnetic characteristics of Ca2+ incorporated superparamagnetic Zn0.5−xCa0.1Co0.4+xFe2O4 (x = 0.0, 0.05 & 0.1) nanoferrites, J Alloys Compd 886 (2021). https://doi.org/10.1016/j.jallcom.2021.161190.
14. B.L. Choudhary, Garima, P.M.Z. Hasan, R. Darwesh, S. Kumar, S. Dalela, S.N. Dolia, P.A. Alvi, Low temperature field dependent magnetic study of the Zn0.5Co0.5Fe2O4 nanoparticles, J Magn Magn Mater 536 (2021). https://doi.org/10.1016/j.jmmm.2021.168102.
15. N. Kumari, Sarita, Anchal, K.K. Palsaniya, S.R. Choudhary, R. Beniwal, Priya, P.M. Saini, S.N. Dolia, P.A. Alvi, P.A. Alvi, B.L. Choudhary, Structural and magnetic behavior in nanocrystalline Ni0.5Co0.5Fe2O4, in: Mater Today Proc, 2021: pp. 289–292. https://doi.org/10.1016/j.matpr.2022.08.241.
16. N. Kumari, Sarita, Anchal, Priya, K.K. Palsaniya, R.K. Beniwal, S.R. Choudhary, M.S. Rulaniya, P.M. Saini, S.N. Dolia, P.A. Alvi, B.L. Choudhary, The role of citric acid for formation of nanocrystalline MnFe2O4 ferrite, Appl Phys A Mater Sci Process 130 (2024). https://doi.org/10.1007/s00339-024-07423-9.
17. Sarita, Anchal, Priya, R.K. Beniwal, M.S. Rulaniya, P.M. Saini, P. Yadav, U. Kumar, Aakansha, P.A. Alvi, P.A. Alvi, B.L. Choudhary, Development and characterization of superparamagnetic Zn-Doped Nickel ferrite nanoparticles, J Magn Magn Mater 610 (2024). https://doi.org/10.1016/j.jmmm.2024.172547.
18. P. Yadav, R.K. Beniwal, Anchal, Sarita, Ritu, S.N. Dolia, P.A. Alvi, B.L. Choudhary, Structural and Morphological Characterization of Cr0.2Ni0.8-xCoxFe2O4 Nanocrystalline Samples Synthesized via Sol-Gel Auto-Combustion Method, in: S. Kumari, A. Singh, B. Tripathi, M. Baboo (Eds.), Proceedings of the 1st International Conference on Materials and Thermophysical Properties, Springer Nature Singapore, Singapore, 2025: pp. 262–266.
19. S. Srivastava, S. Kumar, S. Agrawal, S.S. Sharma, R. Kumar, A. Saxena, B.L. Choudhary, S. Mathur, Y.K. Vijay, Study of structural and gas sensing properties of tantalum coated polyaniline composite thin films, in: AIP Conf Proc, 2011: pp. 765–766. https://doi.org/10.1063/1.3606083.
20. Sarita, Anchal, Priya, S.R. Choudhary, M.S. Rulaniya, A. Kumar, S.N. Dolia, P.A. Alvi, B.L. Choudhary, Studies of Structural, Optical, and Raman Analysis of Ni-Substituted CoFe2O4, Physica Status Solidi (A) Applications and Materials Science 221 (2024) 1–11. https://doi.org/10.1002/pssa.202400083.
21. Anchal, Sarita, Priya, N. Kumari, K.K. Palsaniya, M.S. Rulaniya, P.A. Alvi, S.N. Dolia, B.L. Choudhary, Characterization and synthesis of nanocrystalline CoFe2O4 ferrites prepared by sol-gel method with citric acid variation, in: AIP Conf Proc, 2024. https://doi.org/10.1063/5.0224532.
22. Sarita, Anchal, Priya, N. Kumari, K.K. Palsaniya, M.S. Rulaniya, P.A. Alvi, S.N. Dolia, B.L. Choudhary, Synthesis and characterization of nano-crystalline Ni-doped CoFe2O4ferrite for biomedical applications, in: AIP Conf Proc, 2024. https://doi.org/10.1063/5.0224545.

23. Priya, Sarita, Anchal, N. Kumari, K.K. Palsaniya, M.S. Rulaniya, S.R. Choudhary, R.K. Beniwal, P.M. Saini, P.A. Alvi, S.N. Dolia, B.L. Choudhary, Structural, morphological, and spectroscopic insights into nanocrystalline Mn-doped ZnFe2O4 ferrite for technological applications, in: AIP Conf Proc, 2024. https://doi.org/10.1063/5.0224505.
24. Anchal, Sarita, K.K. Palsaniya, Priya, N. Kumari, S.N. Dolia, P.A. Alvi, B.L. Choudhary, Tailoring quantum dots through citric acid modulation of CoFe2O4 ferrite, Mater Chem Phys 313 (2024). https://doi.org/10.1016/j.matchemphys.2023.128820.
25. B.L. Choudhary, S. Chander, S.N. Dolia, P.A. Alvi, Synthesis of ni- And co- doped ferrite nanoparticles and study of magnetic behaviour with temperature variation, in: AIP Conf Proc, 2020. https://doi.org/10.1063/5.0001167.
26. R.K. Beniwal, P.M. Saini, Sarita, Anchal, Priya, K.K. Palsaniya, S.R. Choudhary, M.S. Rulaniya, N. Kumari, J. Singh, S.N. Dolia, B.L. Choudhary, Synthesis and magnetic properties of polyhedral Fe3O4 nanocrystals, in: AIP Conf Proc, 2024. https://doi.org/10.1063/5.0224484.